Dalton Transactions

ROYAL SOCIETY OF CHEMISTRY

PAPER

View Article Online
View Journal | View Issue

Cite this: *Dalton Trans.*, 2024, **53**, 7880

Enhanced white rot control in garlic bulbil using organic–inorganic hybrid materials as coating membranes†

Lorena Alves de Melo Bessa,*[a] Mariane Luísa Ferreira Nazário,[a] Celly Mieko Shinohara Izumi,[b] Vera Regina Leopoldo Constantino,[c] Valdir Lourenço, Jr.,[d] Everaldo Antônio Lopes,[a] Eduardo Seiti Gomide Mizubuti[e] and Jairo Tronto[a]

Organic–inorganic hybrid materials have a range of applications due to their unique properties. Their application in agriculture brings alternatives for the controlled release of nutrients in the soil, the seed coating, the transport of herbicides, and the treatment of plant diseases. The present study aimed to investigate the use of fungicides incorporated into hybrid membranes formed by synthetic hectorite (LAPONITE®) and polymers in the pre-treatment of garlic bulbils exposed to the pathogen *Stromatinia cepivora*, which causes white rot. The coatings were selected by a germination test, based on the bulbil sprouting index, and by a mycelial growth inhibition test, based on the percentage of mycelial growth inhibition. The chosen membranes were used to coat the bulbils for bioassays conducted in a biochemical oxygen demand incubator at 17 °C. The coated bulbils were planted in soil samples containing three different densities of *Stromatinia cepivora*: 0.1 g, 1.0 g, and 10 g of sclerotium per L of soil. Membranes containing 2% carboxymethyl cellulose and 2% LAPONITE® incorporated with (i) the fungicide tebuconazole (36 mg L^{-1}) and (ii) the combination of the actives tebuconazole (36 mg L^{-1}) and triadimenol (62 mg L^{-1}) showed the total rate of sprouting and null indices of incidence of symptoms and mortality in its repetitions. The hybrid membranes were characterized employing several techniques, including X-ray diffraction, infrared and Raman spectroscopy, thermogravimetric analysis and differential scanning calorimetry coupled to mass spectrometry, and optical microscopy. Characterization data confirmed the presence of fungicides incorporated into the membranes. Some concentrations of fungicides were low enough not to be detected in all analyses performed, although they guaranteed a protective character to the bulbils about the fungus *S. cepivora* present in the soil, with a possibility of antifungal pre-treatment with a potential reduction in the concentration used.

Received 31st January 2024,
Accepted 5th April 2024

DOI: 10.1039/d4dt00301b

rsc.li/dalton

1. Introduction

Garlic (*Allium sativum* L.) is a high-value bulbil plant cultivated worldwide for food flavouring and medicinal purposes because of its therapeutic properties. Although garlic has been cultivated in Brazil for many years, the country still must import about 55% of the garlic it consumes due to high domestic consumption and recurrent crop losses caused by pests, especially the fungus *Stromatinia cepivora* (syn. *Sclerotium cepivorum* Berk.).[1] Such a pest problem has spread to all continents. *Stromatinia cepivora* causes white rot and is considered the greatest threat to Alliaceae crops, including garlic, onion (*Allium cepa* L.), and other related species.[2] White rot first affects the aerial part of the plant, causing the leaves to turn yellow. The lower part of the stem is then attacked by white mycelium, a vegetative part of the *S. cepivora* fungus.[3]

The fungus then develops sclerotia to reserve its food for long periods, even without a host in the soil. Identifying this

[a]*Instituto de Ciências Exatas e Tecnológicas, Universidade Federal de Viçosa, Campus Rio Paranaíba, CEP 38810-000 Rio Paranaíba, MG, Brazil. E-mail: jairotronto@ufv.br*
[b]*Departamento de Química, Instituto de Ciências Exatas, Universidade Federal de Juiz de Fora, Campus Univeritário, CEP 36036-900 Juiz de Fora, MG, Brazil. E-mail: celly.izumi@ufjf.br*
[c]*Departamento de Química Fundamental, Instituto de Química, Universidade de São Paulo, Av. Prof. Lineu Prestes 748, CEP 05508-000 São Paulo, SP, Brazil. E-mail: vrlconst@iq.usp.br*
[d]*Embrapa Hortaliças, CEP 70.351-970 Brasília, Distrito Federal, Brazil. E-mail: valdir.lourenco@embrapa.br*
[e]*Departamento de Fitopatologia, Universidade Federal de Viçosa, Campus Viçosa, CEP 36570-900 Viçosa, MG, Brazil. E-mail: mizubuti@ufv.br*

† Electronic supplementary information (ESI) available. See DOI: https://doi.org/10.1039/d4dt00301b

white mycelium and sclerotia is critical to a reliable diagnosis of white rot.[4]

In addition to preventive measures, fungicides capable of inhibiting sclerotia-producing pathogens have been reported to be effective in controlling white rot. These fungicides are applied directly to bulbils and seedlings before planting, such as procymidone, vinclozolin and iprodione.[3] Furthermore, studies have been carried out to seek biological control of white rot using isolated microorganisms, and techniques such as solarization combined with the use of commercially used fungicides such as triadimenol and tebuconazole have been employed.[5,6]

Several studies have explored the potential of using organic–inorganic hybrid materials as effective alternatives in agricultural applications for managing certain plant diseases. These hybrid materials are homogeneous systems of organic and inorganic components, typically on a nanometre to micrometre scale. The synergy between these components allows for integrating various physical and chemical properties into the material, resulting in enhanced surface area, ion exchange capabilities, biocompatibility, increased durability, and several other advantages.[7,8]

The use of polymeric membranes in the coating of bean seeds (*Phaseolus vulgaris* L.), from organic–inorganic hybrid materials, incorporating 1-naphthaleneacetic acid (NAA), is an example of how these materials have shown good results in the physiological characteristics of the plant, improving its development.[9] Another example has been the use of organic–inorganic hybrid materials in the coating of sugarcane microstalks, to reduce the percentage of stalks used in the crop planting process.[10]

From this perspective, this study focused on preparing organic–inorganic hybrid materials to coat garlic bulbils as a pre-planting treatment. Specifically, the study aimed to (i) prepare organic–inorganic hybrid membranes for coating garlic bulbils using the interaction between LAPONITE®, a biopolymer (alginate or carboxymethyl cellulose), and a fungicide (tebuconazole, triadimenol, or boscalid); (ii) confirm the interaction between fungicides and polymeric membranes using Fourier-transform infrared spectroscopy (FTIR-ATR), Raman spectroscopy, optical microscopy, thermogravimetric analysis (TGA-DSC-MS), and X-ray diffraction (XRD); and (iii) evaluate the effect of bulbils coated with fungicides on the control of *S. cepivora*.

To our knowledge, this is the first study to evaluate the use of CMC and LAPONITE® with fungicides as coating membranes on garlic bulbils to prevent the infection by *S. cepivora*.

2. Experimental section

2.1 Reagents

For the preparation of organic–inorganic hybrid materials, the following reagents were used: LAPONITE® (LAP) was provided by Buntech (São Paulo, Brazil); sodium alginate (ALG) was produced by Êxodo Científica (Sumaré, Brazil); carboxymethylcellulose (CMC), tebuconazole (TB), triadimenol (TD), and boscalid (BC) fungicides were produced by Merck (Darmstadt, Germany); calcium nitrate (NC) was produced by ACS (Rio de Janeiro, Brazil). Deionized water was obtained using a Milli-Q water purification system (Millipore, France).

2.2 Preparation of organic–inorganic hybrid materials for coating garlic bulbils

All solutions and dispersions were kept on a magnetic stirrer to homogenize the phase for the synthesis. The dispersions containing LAPONITE® in their composition were heated on a hot plate at 80 °C and under agitation on a magnetic stirrer for complete solubilization and exfoliation of the clay tactoids.[11] The prepared composites and their respective compositions in terms of the amount of LAP, ALG, and CMC, and fungicidal activity are presented in Table 1.

Table 1 Composition of the membranes

Lap® (mg)	ALG (mg)	CMC (mg)	TD (mg)	TB (mg)	BC (mg)	IP (mg)	V (L)	CODE
—	2000	—	—	—	—	—	0.1	ALG2
—	—	2000	—	—	—	—	0.1	CMC2
2000	2000	—	—	—	—	—	0.2	ALG2-LAP2
2000	—	2000	—	—	—	—	0.2	CMC2-LAP2
—	2000	—	0.62	—	—	—	0.1	ALG2-TD
—	—	2000	0.62	—	—	—	0.1	CMC2-TD
2000	2000	—	0.62	—	—	—	0.2	ALG2-LAP2-TD
2000	—	2000	0.62	—	—	—	0.2	CMC2-LAP2-TD
—	2000	—	—	0.36	—	—	0.1	ALG2-TB
—	—	2000	—	0.36	—	—	0.1	CMC2-TB
2000	2000	—	—	0.36	—	—	0.2	ALG2-LAP2-TB
2000	—	2000	—	0.36	—	—	0.2	CMC2-LAP2-TB
—	2000	—	—	—	0.46	—	0.1	ALG2-BC
—	—	2000	—	—	0.46	—	0.1	CMC2-BC
2000	2000	—	—	—	0.46	—	0.2	ALG2-LAP2-BC
2000	—	2000	—	—	0.46	—	0.2	CMC2-LAP2-BC
—	—	—	—	—	—	5.0×10^7	0.1	CP
—	—	—	0.62	—	—	—	0.1	STD
—	—	—	—	0.36	—	—	0.1	STB
—	—	—	0.62	0.36	—	—	0.1	STD-TB
2000	—	2000	0.62	0.36	—	—	0.2	CMC2-LAP2-TB-TD

2.3 Structural characterization of organic–inorganic hybrid materials

2.3.1 X-ray diffraction (XRD). A Shimadzu model XRD-6000 X-ray diffractometer was used for analysis *via* X-ray diffractometry (XRD). A graphite crystal monochromator selects the radiation used from Cu-Kα_1 with λ = 1.5406 Å. The source's electrical current and potential were 30 mA and 30 kV, respectively. The diffractograms were collected between (2θ) 4° and 70°, with a step of 1.0° per minute.

2.3.2 Molecular absorption spectroscopy in the infrared region with a Fourier transform and attenuated total reflectance (FTIR/ATR) accessory. A Jasco model FTIR 4100 spectrophotometer with an attached ATR accessory was used. The spectra obtained by the analysis were the result of 256 scans with a resolution of 4 cm^{-1} and a wave number range of 4000 to 400 cm^{-1}.

2.3.3 Thermogravimetric analysis and differential scanning calorimetry coupled to mass spectrometry (TGA-DSC-MS). Thermogravimetric analyses were carried out using a 28 Netzsch STA 409 PC – Luxx thermobalance for simultaneous TG-DSC analysis coupled to a Netzsch mass spectrometer model QMS 403 C – Aeölos for detecting gases released from the sample. Approximately 5 mg of sample was placed in an alumina crucible and heated at 10 °C min^{-1} in a synthetic air flow (80% N_2 and 20% O_2) of 100 cm^3 min^{-1}, from 30 °C to 1000 °C.

2.3.4 Vibrational Raman spectroscopy. The spectra were recorded on an FT-Raman spectrometer, model RFS100/S from Bruker Optics, using an Nd:YAG laser with excitation at 1064 nm. The power used was 100 mW, with a resolution of 4 cm^{-1} and 1024 scans.

2.3.5 Light microscopy. Light microscopy images were collected using a stereoscopic microscope (Physis brand) with 40 times magnification, and they were recorded with a cell phone camera. ImageJ® software was used for the calculation of coating thickness.

2.4 Coating of garlic bulbils to evaluate the sprouting rate and formation of the aerial part and root system of plants

The collected bulbils were evaluated for the Visual Dormancy Index (VDI) through longitudinal cuts until germination buds with 50% of the germinating leaves were observed.[12] Then, the bulbils were subjected to vernalization at 4 °C with the relative humidity (RH) between 65% and 70% for 45 days. This process consists of a pre-planting treatment that stimulates the differentiation and formation of the bulbils, even at photoperiods and temperatures inappropriate for the crop.[13]

The vernalized bulbils were kept at room temperature for 24 hours before planting. Subsequently, they were coated with the synthesized solutions. The garlic cloves coated with solutions containing sodium alginate were immersed in a 5.0% Ca $(NO_3)_2$ solution for 10 s to form a hydrogel on the prepared membranes.[14] All the bulbils were dried at room temperature for 2 h before planting them in sandboxes, with the garlic cloves placed vertically, with the bud pointing upwards, in grooves 2 to 3 cm deep. There were 5 planting lines of 3 bulbils each. The experimental design was completely randomized with seven replications.

During the next 15 days after planting, daily monitoring was carried out to identify germination occurrences based on the treatment type, and soil irrigation was carried out as needed to maintain moisture. After the growth period, the roots and aerial parts were washed, dried, and measured separately. The roots were then digitized using a scanner to determine the volume, surface area, and length using Safira® software. The dry and fresh masses of the roots and aerial parts were also quantified on an analytical balance. Principal component and cluster analyses were performed using the R software version 4.04 (R Core Team, 2021) on the variables of height, dry and fresh mass of roots and aerial parts.

2.5 Inhibition tests of mycelial growth of *Stromatinia cepivora* by coating garlic bulbils with fungicides associated with organic–inorganic materials

The active fungicides triadimenol solutions at 62 mg L^{-1}, tebuconazole at 36 mg L^{-1}, and boscalid at 4.6 mg L^{-1} were prepared for the mycelial growth inhibition study. These solutions were used as a basis for preparing the polymeric membranes. The experiment was conducted in a completely randomized design (CRD) with four replications. One replication consisted of a plate containing a plug of *S. cepivora* mycelium and a garlic bulbil on potato dextrose agar (PDA). The positive control was made with the active ingredient iprodione (Magic®, 500 g L^{-1}), traditionally used in garlic cultivation, to compare its inhibitory effect on mycelial growth with the prepared coatings. The negative controls were composed of PDA media without the fungicide and *S. cepivora* mycelium plug (CNM) to evaluate possible contamination of the medium; PDA culture medium with mycelium plug (CNMB) to evaluate fungal growth; and PDA culture medium containing uncoated bulbils, with two repetitions being made (CN1 and CN2) to observe possible contamination in the bulbils used.

Before the experiment, the garlic bulbils were washed in running water and dried at room temperature. They were then immersed for 120 s in a 2% sodium hypochlorite solution to be disinfected and washed again in running water. After preparing the plates, they were kept at 17 °C with a 12-hour photoperiod. The mycelial growth of the fungus was monitored daily. The experiment was terminated when the pathogen grew throughout the plate in the treatment containing only mycelium discs and PDA medium.

2.6 Incidence of white rot in garlic bulbils coated with polymeric membranes and incorporated fungicides

Twenty-seven liters of red latosol were collected and sieved near the campus at coordinates 19°13′04.9″ S 46°13′28.1″ W. Latosol was packed in plastic bags and autoclaved at 120 °C for 60 minutes. It rested for 24 hours and autoclaved again under the same conditions. The sclerotia of *S. cepivora* used in the experiment were obtained from naturally infested soil collected near Rio Paranaíba city at coordinates 19°11′39″ S 46°

14′37″ W. For disinfestation, the sclerotia were immersed in 50% ethyl alcohol (alcohol by volume) for 30 s, followed by immersion in 0.5% v/v sodium hypochlorite for 60 s, rinsing with deionized water and drying on germination paper, previously autoclaved. The sclerotia were kept conditioned for three months and buried to break constitutive dormancy. A volume of 300 g of autoclaved latosol was used for each repetition. In each sample, the soil was first added to half the volume, and then the remaining soil was mixed with the sclerotia, completing the volume of 300 mL of soil. In each cup containing the soil, holes were made at the bottom to absorb water during the cultivation period. The containers were placed in plastic trays and taken to the BOD incubator for subsequent planting of the coated garlic bulbils. The description of the membranes is presented in Table 1. The bulbils were immersed in the membranes for 60 seconds each and dried for 120 min at room temperature. At the end of the drying period, two garlic bulbils were planted per sample, and the trays were kept in a BOD incubator at 17 °C ± 2 °C with a 12 h light photoperiod. The trays were filled with 2 L of distilled water each and checked every 72 h to replace water and monitor growth. The experiment was set up in a completely randomized design with three replications for each experimental unit. A replicate was considered as a container containing two plants.

3. Results and discussion

3.1 Characterization of organic–inorganic hybrid materials

3.1.1 X-ray diffraction analysis. The XRD pattern of LAP showed a broad peak referring to the diffraction of (001) planes at 2θ equal to 6.78°. The LAP's low crystallinity is due to the small particles and low structural organization in the stacking direction.[15] The diffractogram of CMC had a characteristic peak in the 2θ region equal to 20°, while ALG presented an amorphous signal, characterized by the absence of diffraction peaks and a high baseline.[16]

Concerning the fungicidal active ingredients, the XRD pattern of TD showed numerous intense diffraction peaks in the 2θ region between 5° and 45° with a close relationship in width and half height, characteristic of crystalline materials. The active TB presented diffraction peaks between 15° and 45°. However, after mixing with the LAP and the polymer, the diffractograms showed a possible amorphization of the crystalline structures of the active ingredients, which may be related to the low concentration used and/or the interaction of the active ingredients with the amorphous materials present in the films (Fig. 1).

3.1.2 Analysis by molecular absorption spectroscopy in the infrared region with a Fourier transform and attenuated total reflectance (FTIR-ATR) accessory. The FTIR-ATR spectrum of LAP showed a band at 3675 cm^{-1} with low intensity, characteristic of stretching vibrations of Mg–OH groups. In the regions of 3438 cm^{-1} and 1641 cm^{-1}, stretching vibrations are presented as characteristics of hydroxyl groups (OH–) present in the LAPONITE® or water molecules adsorbed by the clay in the hydration process (Fig. 2).

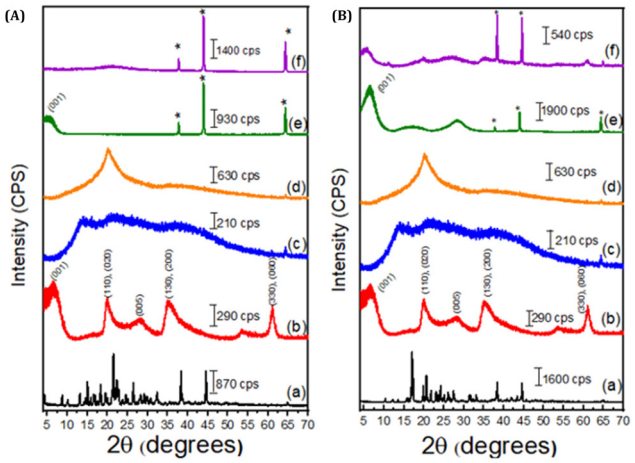

Fig. 1 XRD patterns of (A) – (a) TD; (b) LAP; (c) ALG; (d) CMC; (e) ALG2-LAP2-TD and (f) CMC2-LAP2-TD and (B) – (a) TB; (b) LAP; (c) ALG; (d) CMC; (e) ALG2-LAP2-TB; and (f) CMC2-LAP2-TB. The membrane codes are described in Table 1.

A band of strong intensity evident at 960 cm^{-1} corresponds to the stretching vibrations of the Si–O bonds present in the molecule. In the region of 652 cm^{-1}, a band of medium intensity occurs due to stretching vibrations characteristic of Mg–OH–Mg type bonds in the structure.

Finally, a band at 425 cm^{-1} is attributed to the presence of Si–O–Mg and Si–O–Si bonds in the structure due to the proximity and overlap of the bands in the spectrum.[17,18]

The sodium alginate (ALG) spectra present a broad band of average intensity in the region of 3401 cm^{-1}, corresponding to the presence of –OH bonds in the polymer structure and the region of 2928 cm^{-1}, associated with the stretching vibrations of $-CH_2$. The bands at 1079 cm^{-1} and 1018 cm^{-1} are characteristic of the CO and CO–C vibrations in mannuronic and

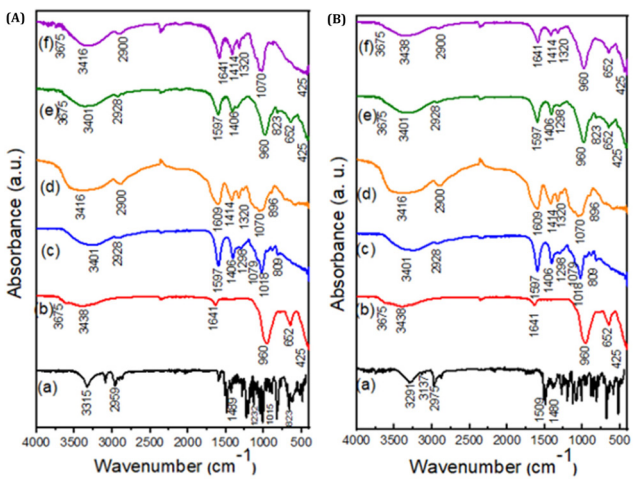

Fig. 2 FTIR-ATR spectra for (A) – (a) TD; (b) LAP; (c) ALG; (d) CMC; (e) ALG2-LAP2-TD; and (f) CMC2-LAP2-TD and (B) – (a) TB; (b) LAP; (c) ALG; (d) CMC; (e)ALG2-LAP2-TB; and (f) CMC2-LAP2-TB. The membrane codes are described in Table 1.

guluronic monomers, respectively. The band in the region of 809 cm^{-1} evidences the presence of guluronic acid monomers. In sodium carboxymethylcellulose (CMC) spectra, the strong band at 3416 cm^{-1} indicates the stretching vibrations of –OH bonds in the intramolecular and intermolecular structures of carboxymethylcellulose molecules. The band of strong intensity in the region of 1609 cm^{-1} occurs due to the presence of sodium carboxylate ($COO^{-}Na^{+}$) in the molecule, and the neighboring bands at 1414 cm^{-1} and 1320 cm^{-1} are characteristic of the presence of CO bonds in the group's carboxylic acid molecule.

The triadimenol spectra present a strong band at 3315 cm^{-1}, characteristic of chlorine directly linked to the aromatic ring, in addition to cyclic nitrogen in the composition of the molecule. Triadimenol is a fungicide from the triazole class with the presence of cyclic bonds composed of nitrogen, therefore presenting a strong band at 1489 cm^{-1}.[19]

As it is an aromatic ether, a band of strong intensity is evident at 1232 cm^{-1} and another one at 1015 cm^{-1}, characteristic of the presence of C–O bonds in ethers. Due to the two substituents on the aromatic ring being in the *para* position, there is a band of strong intensity at 823 cm^{-1}.

The spectra of tebuconazole indicate vibrations in the region of 3291 cm^{-1} related to the presence of an –OH bond in the molecule and also show stretching of C–H bonds with the aromatic ring at 3137 cm^{-1} and symmetric stretching referring to methyl groups ($-CH_3$) in the band at 2975 cm^{-1}.[20] In the region of 1509 cm^{-1}, a characteristic vibration occurs in the connection between the benzene ring and carbon. The strong band evident at 1486 cm^{-1} refers to the vibration of the carbons present in the aromatic ring, a phenomenon known as skeleton vibration.

3.1.3 Thermogravimetric analysis with differential scanning calorimetry and mass spectrometry (TGA-DSC-MS). The thermograms presented in the ESI† revealed that both the membranes synthesized with sodium alginate and those with sodium carboxymethylcellulose each presented two major decomposition events during the heating program carried out (from 30 °C to 1000 °C) – Fig. S1.† The first event occurred between 200 and 300 °C, characteristic of the decomposition of compounds by volatilization, with an average loss of 40% of the mass with molar mass m/z = 18, which indicates water as the main decomposition product. The second event, between 500 and 700 °C, characteristic of the decomposition of "carbon black", with a molar mass m/z = 44, determined using the mass spectrometer, indicates a loss of 30% in mass of CO_2 molecules in both polymer structures in this temperature range. Differentially, it was found that the heat flow was predominantly endothermic, that is, heat is supplied to the sample to maintain the temperature difference between the sample and the reference null.

The DTG curves presented indicated the starting temperatures of the decomposition reactions and the moments at which the reaction rates became maximum during the process. Sharp peaks were observed at the same temperatures for the main decomposition events presented in the TG curves.

From 700 °C onwards, there was a stage of waste decomposition, in which the formation of zinc and aluminum oxides generally occurs. The thermogravimetric curves allowed the evaluation of the thermal stability of the constituent materials, the water content in the compounds, and the chemical composition of the samples.

3.1.4 Vibrational Raman spectroscopy analysis. The Raman spectrum of pure LAPONITE® presents a band of strong intensity at 684 cm^{-1} due to the symmetric vibrations of the SiO_4 networks present in the synthetic clay structure and bands of lower intensity at 1087 cm^{-1}, associated with the presence of asymmetric Si–O bonds: 362 cm^{-1}, coming from vibrational modes characteristic of Si–O and Mg–O bonds, and 188 cm^{-1}, coming from vibrations of $MgLiO_6$ groups, present in the octahedral interlayer of the clay.[21–23] The spectra of the hybrid materials present the band at 684 cm^{-1} a characteristic of LAPONITE® that confirms the presence of clay (Fig. 3).

The Raman spectrum of triadimenol presents a band of strong intensity between 1500 cm^{-1} and 1600 cm^{-1}, as also seen in the active tebuconazole, referring to the chemical group of triazoles. At 1596 cm^{-1}, there is a band referring to cyclic nitrogen bonds. The active ingredient also presents bands of strong intensity between 1200 cm^{-1} and 1300 cm^{-1}, characteristic of the aromatic ether present in the structure. In the region of 1373 cm^{-1}, there is a strong band of high intensity characterized by the *-para* position of the substituents of the aromatic ring of the triadimenol. Other characteristic active bands are also found at 1120 cm^{-1} and range from 950 cm^{-1} to 600 cm^{-1}.

The sodium alginate polymer has two bands, at 1416 cm^{-1} and 1614 cm^{-1}, characteristic of the stretching vibrations of the COO-carboxylic bonds. At 1096 cm^{-1}, a strong band highlights the presence of C–C stretching vibrations, C–O–C glycosidic bonds, and symmetric stretching vibrations known as "ring breathing".

After synthesis, bands around 1600 cm^{-1}, 1400 cm^{-1}, and 1100 cm^{-1} indicate the presence of sodium alginate. The 1614 cm^{-1} band underwent a shift to 1608 cm^{-1}, which can be justified by the molecular interactions between the polymer and the active triadimenol fungicide. The same was observed with the 1614 cm^{-1} band, which moved to 1594 cm^{-1} in relation to the interaction of sodium alginate with the active fungicide tebuconazole.

The Raman spectrum for sodium carboxymethylcellulose has bands like those found in the sodium alginate molecule, such as the vibrational modes of symmetric and asymmetric stretching of the carboxylate ion, respectively, found at 1415 cm^{-1} and 1599 cm^{-1}. Likewise, a band at 1099 cm^{-1} highlights the presence of C–C stretching vibrations, C–O–C glycosidic bonds and the symmetric stretching vibrations of "ring breathing".

The Raman spectrum of tebuconazole presents bands characteristic of the fungicide gathered in the region between 1590 cm^{-1} and 1800 cm^{-1}, mainly due to a band of strong intensity at 1596 cm^{-1}, which highlights the presence of the compound. The band between 1500 cm^{-1} and 1600 cm^{-1} is

characteristic of the group of triazoles, heterocyclic compounds formed by the presence of 3 nitrogen atoms in the same cyclic nucleus.

The absence of a Raman signal referring to the fungicide molecules in the spectra of the hybrid materials is associated with the low doses used compared to those in commercial use. Furthermore, changes in the spectra profiles of the synthesized membranes containing fungicides were observed in relation to those without fungicides. These subtle changes in profiles suggested an interaction between the fungicidal actives and the polymers in the membranes.

3.2 Effect of coatings on the sprouting rate and formation of the aerial part and root system of plants

Garlic bulbils coated with membranes that contained CMC2-LAP2 in their composition showed the highest sprouting rates of 86% and 100%, respectively. In addition to sprouting indices, the coatings were evaluated in relation to uniformity, viscosity, and flow on the surface of the bulbils. From the analysis of the synthesized coatings, the treatments selected were ALG2, CMC2, ALG2-LAP2, and CMC2-LAP2. The four coatings together with the control (BR) were evaluated in relation to germination percentage and shoot length. Regarding the development of the aerial part, seedlings from bulbils coated with hybrid materials showed the highest length values. The coating CMC2-LAP2 showed 49.6% higher growth than the control (BR). According to the germination percentages observed, it is possible to suggest that the coatings used supported the germination process, as well as the development of the seedlings, in contrast to the bulbils that did not receive any type of treatment. In fact, seed coating can significantly help increase bulbil vigor, reflecting cultivar growth and providing seed protection and crop maintenance.[20]

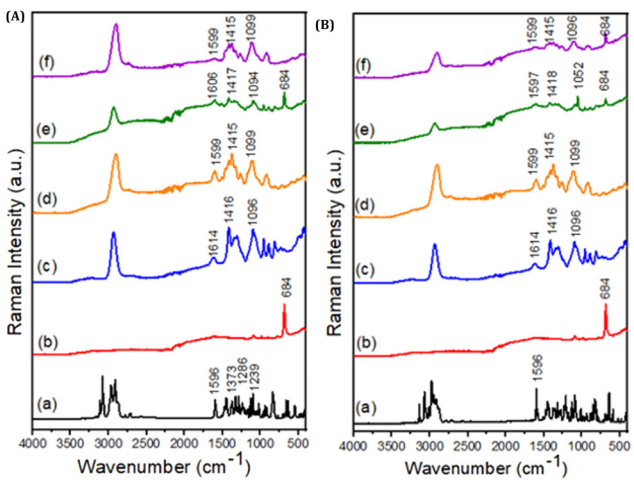

Fig. 3 Raman spectra for: (A) – (a) TD; (b) LAP; (c) ALG; (d) CMC; (e) ALG2-LAP2-TD; and (f) CMC2-LAP2-TD and (B) – (a) TB; (b) LAP; (c) ALG; (d) CMC; (e)ALG2-LAP2-TB; and (f) CMC2-LAP2-TB. The membrane codes are described in Table 1.

3.3 Effect of garlic bulbil coatings on the inhibition of mycelial growth of *Stromatinia cepivora*

The treatments based on the active ingredient tebuconazole obtained the highest average percentages of inhibition of mycelial growth and allowed lower average growth of mycelium discs on the plates in relation to the other fungicidal active ingredients tested. Among the treatments using the active ingredient, the CMC2-LAP2-TB coating was the one that showed the highest percentage of growth inhibition – PIC (64.5%), as well as the lowest *S. cepivora* colony area (68.3 cm^2), having a significant inhibitory behaviour considering the low concentration of the fungicidal active ingredient added to the coating (36 mg L^{-1}) – Fig. S2.† As is known, tebuconazole is a triazole fungicide widely used to control *S. cepivora* in other species of the Allium family.[24]

Comparing results from using tebuconazole with other fungicides in mycelial growth inhibition tests, it was found that tebuconazole also showed greater inhibitory efficiency, which may be related to the molecular structure of the active ingredient.[25] The use of the active ingredient tebuconazole with its antifungal activity combined with the organic–inorganic hybrid material covering the bulbils may have intensified the protection offered to the bulbils against external agents, leading to a reduction in mycelial growth and consequently, a greater area of inhibition in relation to growth from *S. cepivora.*

In contrast, garlic bulbils coated only with organic–inorganic hybrid materials, without the presence of fungicides, did not inhibit the mycelial growth of *S. cepivora*, nor was any inhibition observed from coatings containing the fungicide boscalid, which may be related to the low concentration used (4.6 mg L^{-1}) and its low fixation in the coatings in which it was incorporated. Table 2 presents the areas of mycelial growth and the percentages of mycelium growth inhibition rate (MGIR) for each treatment. In the positive control, garlic bulbils treated with the active fungicide iprodione showed an inhibitory effect of 87.7% when a commercial dose of 1.0 kg of the product per 100 kg of bulbils was used, proportional to the weight of the seeds for application. It is worth remembering that the concentration of the active tebuconazole used in the synthesis of the coatings (36 mg L^{-1}) was 5555.5 times lower than that used commercially (200 g L^{-1}). Therefore, studying this active concentration applied to organic–inorganic hybrid materials may suggest an efficient activity of polymeric membranes in contrast to the dose of the commercial product used.

3.4 Evaluation of the inhibitory effect of coatings on soil infested by *Stromatinia cepivora*

At this stage, the coatings were evaluated according to sprouting rates, the incidence of symptoms characteristic of white rot, and mortality during the bioassay. Table 3 shows 30 different treatments evaluated at sclerotium concentrations of 0.1, 1.0, and 10 g L^{-1} of soil.

The sprouting rates were lower for the bulbils that did not receive coatings and were simply immersed in solutions of

Table 2 Effect of the treatments and mycelium growth inhibition rate (MGIR) of *Stromatinia cepivora*

Fungicide used	Treatment	Composition of treatments	Area (cm^2)	MGIR (%)
—	1.1 - 1.4	Untreated garlic bulbil	192.0	0.0
—	2.1 - 2.4	2% sodium alginate solution	192.0	0.0
—	3.1 - 3.4	2% carboxymethylcellulose solution	192.0	0.0
—	4.1 - 4.4	2% sodium alginate and 2% LAPONITE® dispersion	192.0	0.0
—	5.1 - 5.4	2% carboxymethylcellulose and 2% LAPONITE® dispersion	192.0	0.0
Triadimenol	6.1 - 6.4	Untreated garlic bulbil	131.5	31.5
Triadimenol	7.1 - 7.4	2% sodium alginate solution	133.7	30.4
Triadimenol	8.1 - 8.4	2% carboxymethylcellulose solution	116.9	39.1
Triadimenol	9.1 - 9.4	2% sodium alginate and 2% LAPONITE® dispersion	161.5	15.9
Triadimenol	10.1 - 10.4	2% carboxymethylcellulose and 2% LAPONITE® dispersion	145.7	24.1
Boscalid	11.1 - 11.4	Untreated garlic bulbil	192.0	0.0
Boscalid	12.1 - 12.4	2% sodium alginate solution	192.0	0.0
Boscalid	13.1 - 13.4	2% carboxymethylcellulose solution	192.0	0.0
Boscalid	14.1 - 14.4	2% sodium alginate and 2% LAPONITE® dispersion	192.0	0.0
Boscalid	15.1 - 15.4	2% carboxymethylcellulose and 2% LAPONITE® dispersion	192.0	0.0
Tebuconazole	16.1 - 16.4	Untreated garlic bulbil	110.7	42.4
Tebuconazole	17.1 - 17.4	2% sodium alginate solution	114.7	40.4
Tebuconazole	18.1 - 18.4	2% carboxymethylcellulose solution	88.0	54.2
Tebuconazole	19.1 - 19.4	2% sodium alginate and 2% LAPONITE® dispersion	141.2	26.5
Tebuconazole	20.1 - 20.4	2% carboxymethylcellulose and 2% LAPONITE® dispersion	68.3	64.5
Iprodione	21.1 - 21.4	Untreated garlic bulbil (positive control)	23.7	87.7
—	22	Petri dish containing PDA medium (negative control)	0.5	99.8
—	23	Petri dish containing PDA medium and mycelium disc (negative control)	192.0	0.0
—	24	Petri dish containing PDA medium and untreated garlic bulbil (negative control)	0.0	100.0

active fungicides or planted without any pre-treatments. It is worth noting that all bulbils treated with the fungicide iprodione used as a positive control showed a sprouting rate of 100%. This may be related to the activity of iprodione on the soil microbial community, reducing the fungal biomass present in the samples.[26]

Regarding the percentage incidence of symptoms characteristic of white rot, the experiments with a concentration of 0.1 g of sclerotium per L of soil presented the lowest average incidence (8.33%). This must be related to the low concentration of the sclerotia in the soil, which may have contributed to the lack of symptoms in the seedlings.

In the experiments carried out at a concentration of 1 g of sclerotium per L of soil, the CMC2-LAP2-TB-TD coating was the only one which showed no evidence of infection by the fungus in the roots and bulbils.

At the highest concentration of sclerotium tested (10 g of sclerotium per L of soil), two coatings, CMC2-LAP2-TB and CMC2-LAP2-TB-TD, prevented the incidence of symptoms. Correlating these results with those obtained in the mycelial growth inhibition test, the presence of the fungicide tebuconazole in the composition of the polymeric membranes resulted in a greater antifungal effect than that of the other active fungicides used.

Bulbil mortality, a common occurrence in plants affected by white rot, was the highest on average (26.67%) when the bulbils developed in soil with a high concentration of sclerotium (10 g of sclerotium per L of soil).

Bioassay data were analyzed using analysis of variance (ANOVA) with the aid of R software version 4.1.2. Fig. 4 presents the interaction graphs obtained through the relationship between the density of sclerotia in the soil (g of sclerotium per L of soil) and the sprouting, incidence, and mortality rates, respectively.

In Fig. 4(A), all treatments present a sprouting index greater than 33.33% in the sclerotium concentrations in the soil analyzed, except for the negative control (treatment 10 – soil without garlic bulbil). As previously mentioned, the positive control made with the active ingredient iprodione (treatment 9 – garlic bulbil soaked in iprodione solution) showed a sprouting rate of 100% at all sclerotium densities.

Treatments 4 (CMC2-LAP2-TD), 6 (CMC2-LAP2-TB), and 8 (CMC2-LAP2-TB-TD) showed a sprouting rate greater than 83.33% at densities of 1.0 and 10.0 g of sclerotium per L of soil, being the coatings that obtained the best results at these sclerotium densities in the soil. This may be related to the interaction between the incorporated fungicidal active ingredients and the polymeric membranes composed of 2% CMC and 2% LAPONITE®.

For treatments 1 (untreated garlic bulbil) and 2 (CMC2-LAP2), both without the incorporation of fungicides, a similar behavior was observed in the sprouting, incidence, and mortality, with seed development only at low sclerotium density (0.1 g of sclerotium per L of soil).

Considering Fig. 4(B), which shows the percentages of the incidence of symptoms in relation to the density of sclerotia in the soil, membranes 4, 6 and 8 presented 16.67% (treatment 4) and 0% (treatments 6 and 8) at a density of 10.0 g of sclerotium per L of soil. These percentages are higher than those presented by the positive control (treatment 9), which had a 33.33% incidence at this concentration.

In Fig. 4(C), which indicates the percentages of mortality observed in the experiment, only treatments 6 and 8 obtained zero seedling mortality rates, which suggests a more signifi-

Table 3 Conditions used for the final bioassay

Sclerotium concentration in soil (escl. per g of soil)	Fungicidal active ingredient concentration (mg L^{-1})	Treatment	Treatment composition
0.01	—	1.1 - 1.3	Untreated garlic bulbil
	—	2.1 - 2.3	2% carboxymethylcellulose and 2% LAPONITE® solution
	62.0	3.1 - 3.3	Garlic bulbil soaked in triadimenol solution
	62.0	4.1 - 4.3	2% Carboxymethylcellulose solution and 2% LAPONITE® from triadimenol solution (62 mg L^{-1})
	36.0	5.1 - 5.3	Garlic bulbil soaked in tebuconazole solution
	36.0	6.1 - 6.3	2% carboxymethylcellulose solution and 2% LAPONITE® from tebuconazole solution (36 mg L^{-1})
	62.0 36.0	7.1 - 7.3	Garlic bulbil soaked in combined solution of triadimenol (62 mg L^{-1}) and tebuconazole (36 mg L^{-1})
	62.0 36.0	8.1 - 8.3	2% carboxymethylcellulose solution and 2% LAPONITE® from a combined solution of triadimenol (62 mg L^{-1}) and tebuconazole (36 mg L^{-1})
	1 kg of active ingredient per 100 kg of garlic	9.1 - 9.3	Garlic bulbil soaked in iprodione solution (positive control)
	—	10.1 - 10.3	Soil without garlic bulbils (negative control)
0.1	—	11.1 - 11.3	Untreated garlic bulbil
	—	12.1 - 12.3	2% carboxymethylcellulose and 2% LAPONITE® solution
	62.0	13.1 - 13.3	Garlic bulbil soaked in triadimenol solution
	62.0	14.1 - 14.3	2% carboxymethylcellulose solution and 2% LAPONITE® from triadimenol solution (62 mg L^{-1})
	36.0	15.1 - 15.3	Garlic bulbil soaked in tebuconazole solution
	36.0	16.1 - 16.3	2% carboxymethylcellulose solution and 2% LAPONITE® from tebuconazole solution (36 mg L^{-1})
	62.0 36.0	17.1 - 17.3	Garlic bulbil soaked in combined solution of triadimenol (62 mg L^{-1}) and tebuconazole (36 mg L^{-1})
	62.0 36.0	18.1 - 18.3	2% carboxymethylcellulose solution and 2% LAPONITE® from a combined solution of triadimenol (62 mg L^{-1}) and tebuconazole (36 mg L^{-1})
	1 kg of active ingredient per 100 kg of garlic	19.1 - 19.4	Garlic bulbil soaked in iprodione solution (positive control)
	—	20.1 - 20.3	Soil without garlic bulbils (negative control)
1.0	—	21.1 - 21.3	Untreated garlic bulbil
	—	22.1 - 22.3	2% Carboxymethylcellulose and 2% LAPONITE® solution
	62.0	23.1 - 23.3	Garlic bulbil soaked in triadimenol solution
	62.0	24.1 - 24.3	2% Carboxymethylcellulose solution and 2% LAPONITE® from triadimenol solution (62 mg L^{-1})
	36.0	25.1 - 25.3	Garlic bulbil soaked in tebuconazole solution
	36.0	26.1 - 26.3	2% Carboxymethylcellulose solution and 2% LAPONITE® from tebuconazole solution (36 mg L^{-1})
	62.0 36.0	27.1 - 27.3	Garlic bulbil soaked in a combined solution of triadimenol (62 mg L^{-1}) and tebuconazole (36 mg L^{-1})
	62.0 36.0	28.1 - 28.3	2% carboxymethylcellulose solution and 2% LAPONITE® from a combined solution of Triadimenol (62 mg L^{-1}) and tebuconazole (36 mg L^{-1})
	1 kg of active ingredient per 100 kg of garlic	29.1 - 29.3	Garlic bulbil soaked in iprodione solution (positive control)
	—	30.1 - 30.3	Soil without garlic bulbils (negative control)

cant antifungal potential of these membranes in relation to the others.

Thus, the polymeric membranes synthesized with the combination of CMC and LAPONITE® showed more significant interactions with the active fungicides triadimenol and tebuconazole, resulting in a greater inhibitory effect on the activity of the fungus *S. cepivora* in garlic bulbils. These films were quantified by High-Performance Liquid Chromatography (HPLC) in relation to the amount of fungicidal active ingredient present per film area, showing a dosage of 0.17 mg cm^{-2} in relation to that of triadimenol and 0.098 mg cm^{-2} in relation to that of tebuconazole in the analyzed membranes.

The biocompatibility and non-toxicity of the organic–inorganic hybrid materials that make up the coating, together with the low concentration of fungicides used in the composition of the polymeric membrane, give the material an innovative character for the treatment of pre-planting garlic bulbils.[27–29] Furthermore, using antifungal hybrid materials increases the treatment surface area of the bulbil, while enhancing the inhibitory effect despite reduced quantities and concentrations.[30,31]

It is worth remembering that the bulbils were developed in a BOD incubator at a temperature and photoperiod favorable to the fungus *S. cepivora* throughout the experiment. The presence of water and adequate temperature, humidity, and light photoperiod, among other characteristics, make the environment favorable for fungal development and growth.[32–34]

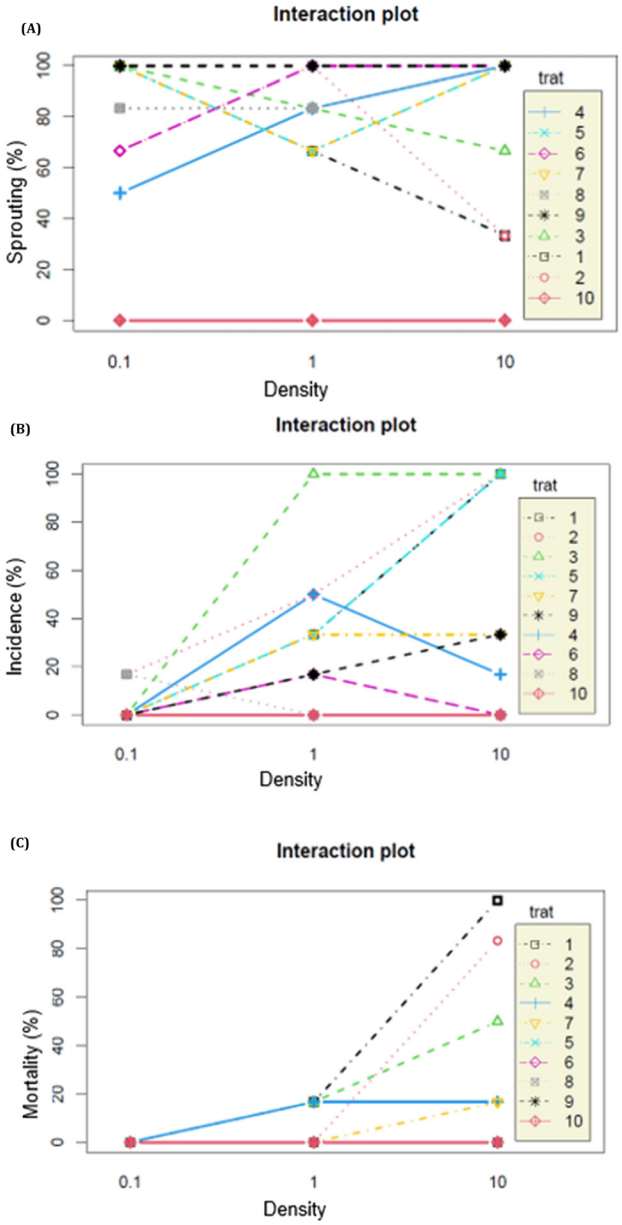

Fig. 4 Interaction graph between the density of sclerotia in the soil (g of sclerotium per L of soil) and (A) the sprouting rates, (B) the incidence rates and (C) the mortality rates observed in the bioassay. The treatment codes and their repetitions are described in Table 3.

4. Conclusions

The use of the fungicides triadimenol and tebuconazole incorporated into polymeric membranes in the coating of garlic bulbils (*Allium sativum* L.) helped mitigate the occurrence of white rot caused by the fungus *Stromatinia cepivora* in the experiments carried out.

The characterization techniques used during this study confirmed the presence of polymeric membranes on the surfaces of garlic bulbils (*Allium sativum* L.) and the interaction between the fungicidal active ingredients and the polymeric membranes that make up the bulbils' coating, highlighting polymer–clay interactions and fungicides.

Although the active fungicides were incorporated at low concentrations, when compared to those used commercially, they showed an inhibitory effect on the mycelial growth of the fungus *S. cepivora*, preventing the appearance of symptoms both in the mycelial growth inhibition test stage – ICM and in the bioassay conducted at BOD.

Among some of the limitations found in the study, the low water solubility of the fungicidal active ingredients led to the investigation of the inhibitory behaviour of the active ingredients at these concentrations in this work, which fortunately showed positive results.

The results presented in this study have opened a discussion on the possibility of potentially reducing the concentrations of fungicidal active ingredients currently used to mitigate white rot disease, based on the associated use of polymeric membranes in the pre-treatment of garlic bulbils (*Allium sativum* L.) and of other potentially affected crops, which implies the need for future studies that investigate the behaviour of this pre-treatment in situations where crops are affected by the fungus *S. cepivora*.

Author contributions

L. A. M. B: conceptualization, investigation, data curation, methodology and writing – original draft. J. T: resources, investigation and supervision, review, and editing. M. L. F. N.: methodology and project contributions. V. R. L. C.: review and editing. V. L. J.: review and editing.

Conflicts of interest

The authors declare no competing interests.

Acknowledgements

Lorena Alves de Melo Bessa gratefully acknowledges the Coordenação de Aperfeiçoamento de Pessoal de Nível Superior – CAPES (Process Number: 88887.678485/2022-00). Dr Tronto thanks Fundação de Amparo à Pesquisa de Minas Gerais – FAPEMIG (Process Numbers: APQ-03410-22 and RED-00056-23). The authors are grateful to the Federal University of Juiz de Fora and the Federal University of São Paulo for providing different characterization techniques used in this study. Dr Tronto and MSc. Lorena Alves de Melo Bessa gratefully acknowledge the Federal University of Viçosa, Rede Mineira de Química (RQ-MG) and the Programa de Pós-Graduação Multicêntrico em Química de Minas Gerais (PPGMQ-MG), for the structuring and support of the research.

References

1 F. V. Resende, *Hortaliças em Revista*, 2018, **7**, 16–17.
2 V. L. Júnior, B. S. Vieira, E. A. Lopes and O. N. Villalta, *Científica*, 2018, **46**, 3.
3 F. J. Crowe, in: *White rot* ed. H. F. Schwartz and K. Mohan, American Phytopathological Society Press, 2008, pp. 22–26; M. Faustini, L. Nicole, E. Ruiz-Hitzky and C. Sanchez, *Adv. Funct. Mater.*, 2018, **28**(27), 30.
4 R. B. Pereira and V. R. Oliveira, *Embrapa Hortaliças-Artigo de divulgação na mídia (INFOTECA-E)*, 2013.
5 M. M. Amin and M. F. A. Ahmed, *Egypt. J. Biol. Pest. Control*, 2023, **33**(1), 27.
6 O. M. Darwesh, M. Osama, *et al.*, *Egypt. J. Chem.*, 2022, **65**(131), 1345–1351.
7 A. Sharma, *et al.*, *Bioact. Mater.*, 2023, **24**, 535–550.
8 J. Brendlé, *Dalton Trans.*, 2018, **47**(9), 2925–2932.
9 V. A. De Castro, *et al.*, *Beilstein J. Nanotechnol.*, 2020, **11**, 1082–1091.
10 A. L. A. Gomes, *Universidade Federal de Viçosa – Dissertação*, 2021, 96.
11 M. Ghadiri, W. Chrzanowski, W. H. Lee, A. Fathi, *et al.*, *Appl. Clay Sci.*, 2013, **85**, 64–73.
12 V. Lourenço Jr., *Científica*, 2018, **46**, pp. 241–256.
13 G. B. De Queiroz, *et al.*, Embrapa Hortaliças, 2016.
14 T. L. Da Silva, *et al.*, *Biol. Act. Appl. Mar. Polysaccharides*, 2017, 57–86.
15 M. D. E. Pinto, R. G. L. Gonçalves, R. M. M. Dos Santos, E. A. Araujo, *et al.*, *Microporous Mesoporous Mater.*, 2016, **225**, 342–354.
16 V. C. F. Burgardt, *J. Food Nutr. Res.*, 2012, **51**, 4.
17 H. Palkova, J. Madejova, M. Zimowska and E. M. Serwicka, *Microporous Mesoporous Mater.*, 2010, **127**(3), 237–244.
18 R. Suzuki, Y. Yamauchi and Y. Sugahara, *Dalton Trans.*, 2022, **51**, 13145–13156.
19 S. D. Martinho, *et al.*, *Int. J. Environ. Res. Public Health*, 2022, **19**(9), 5610.
20 E. L. Martins, *et al.*, *Abstr. Pap. Am. Chem. Soc.*, 2014, 1.
21 V. R. R. Cunha, F. Lima, V. Y. Sakai, L. M. C. Veras, *et al.*, *RSC Adv.*, 2017, **7**(44), 27290–27298.
22 R. R. Domeneguetti, *et al.*, *Appl. Clay Sci.*, 2023, **234**, 106851.
23 N. Iturrioz-Rodriguez, R. Martin-Rodriguez, C. Renero-Lecuna, F. Aguado, *et al.*, *Appl. Surf. Sci.*, 2021, **537**, 10.
24 P. Marín, *et al.*, *Int. J. Food Microbiol.*, 2013, **165**(3), 251–258.
25 L. B. Domingos, *Summa Phytophathologica*, 2018, **44**, 1–5.
26 G. G. Miñambres, *et al.*, *World J. Microbiol. Biotechnol.*, 2010, **26**(1), 161–170.
27 B. Gottardo, *et al.*, *ACS Biomater. Sci. Eng.*, 2023, **9**(12), 6870–6879.
28 M. S. Savelena, *et al.*, *Front. Chem.*, 2019, **7**, 179.
29 F. Ali, *et al.*, *Curr. Nanomater.*, 2016, **1**(2), 83–95.
30 H. Azeredo, *et al.*, *J. Food Sci.*, 2009, **74**(5), 31–35.
31 K. L. Mclean, *et al.*, *Crop Prot.*, 2012, **33**, 94–100.
32 P. Tripathi and N. K. Dubey, *Postharvest Biol. Technol.*, 2004, **32**(3), 235–245.
33 J. R. Coley-Smith, C. M. Mitchell and C. E. Sansford, *Plant Pathol.*, 1990, **39**(1), 58–69.
34 B. M. Cook, *The epidemiology of plant diseases*, 2006, pp. 43–80.